Gulf of Mexico Science

Volume 26
Number 1 *Number 1*

Article 2

2008

Analysis of Secchi Depths and Light Attenuation Coefficients in the Louisiana-Texas Shelf, Northern Gulf of Mexico

A. Lugo-Fernández
Physical Sciences Unit, New Orleans

M. Gravois
Mapping and Automation Unit, New Orleans

T. Montgomery
Mapping and Automation Unit, New Orleans

DOI: 10.18785/goms.2601.02

Gulf of Mexico Science, 2008(1), pp. 14–27

Analysis of Secchi Depths and Light Attenuation Coefficients in the Louisiana–Texas Shelf, Northern Gulf of Mexico

A. Lugo-Fernández, M. Gravois, and T. Montgomery

We analyzed Secchi depths (*Zs*), scalar downwelling irradiance, and transmissometer data collected during 10 cruises that spanned two and one-half years (May 1992–Nov. 1994) over the Louisiana–Texas shelf. The *Zs* increases from the inner shelf (depths ≤ 50 m) to the outer shelf and from nonsummer (*Zs* = 10 m) to summer (*Zs* = 14 m). These changes in Zs are induced by the shelf's circulation and freshwater input, both of which vary seasonally, i.e., nonsummer to summer. Optical parameters (e.g., *Zs*), like the circulation, divide the shelf into an inner and outer shelf along the 50-m isobath. The inner shelf contains turbid waters with low levels of light penetration and large attenuation coefficients that decrease from nonsummer to summer. The outer shelf contains clearer water with high levels of light penetration and small attenuation coefficients year round. Linear regressions between the attenuation coefficients and *Zs* conform to theory and vary seasonally. The scalar downwelling attenuation coefficient and *Zs* are inversely related with coefficients of 1.36 in summer and 1.22 in nonsummer. The beam attenuation coefficient and *Zs* are also inversely related with coefficients of 6.16 in summer and 5.54 in nonsummer.

Photosynthesis is driven by light of wavelengths between 400 and 700 nm. Radiation between these wavelengths (400–700 nm) coincides with visible light and is denoted as the photosynthetically available or active radiation (PAR). In marine environments the horizontal and vertical distributions of PAR are very important to studies of food-web dynamics and optical oceanography.

Many studies have confirmed that PAR decays exponentially with depth (e.g., Jerlov, 1968) and this decay is governed by the scalar downwelling attenuation coefficient (K_0). In practical terms, K_0 measures the clarity or transparency of water to PAR. Because K_0 relates the near-surface PAR to light at depth, it is an important parameter for bio-optical studies (Smith and Baker, 1984). Modern researchers employ two instruments to estimate K_0: a scalar downwelling irradiance meter or a Secchi disk. The first and preferred method is to measure a vertical profile of PAR using a scalar downwelling irradiance meter and estimate K_0 using a least squares regression. This technique is fast and accurate. However, scalar downwelling irradiance meters can be expensive. The second instrument, a Secchi disk, has been in use since the late 19th century (Preisendorfer, 1986; Krezel and Sagan, 1991). Secchi measurements consist of lowering a 30-cm white disk until it disappears and recording the depth of disappearance or Secchi depth (*Zs*) and estimating K_0 using the following equation:

$$K_0 = \frac{1.7}{Zs} \qquad (1)$$

(e.g., Poole and Atkins, 1929; Idso and Gilbert, 1974). However, Holmes (1970) found that in turbid waters the constant in Equation 1 is 1.44.

Despite its simplicity and theoretical limitations (see Preisendorfer, 1986), the Secchi disk is still employed by many researchers because of its low cost, ease of use, and effectiveness in assessing light conditions in a water body. Primary uses of the Secchi disk are to provide an index of trophic activity in the water column, to assess growth and decay of aquatic plant life when long-term observations are available, and as a useful index to visually track movement of suspended detritus (Preisendorfer, 1986; Sanden and Håkansson, 1996).

Optical research in the Gulf of Mexico has revolved around the central topic of freshwater influence on light, which is not surprising given the large inputs of river runoff by the Mississippi River and other smaller rivers. Although early studies were temporally and spatially limited, the paramount effects of freshwater on the light field were recognized. For example, Clarke (1938), Curl (1959), and Højerslev (1985) identified the following trends: that light attenuation decreased in the offshore direction in direct association with freshwater input [high river runoff, high attenuation coefficients (K_0 ~ 0.22–0.45 m^{-1}), low freshwater input equated with low light attenuation], that there was a surface layer of turbid water overlaying clearer water ($K_0 \leq 0.1\ m^{-1}$), and that inorganic and biological particles influence the vertical distribution of K_0. Optical studies over the shelf and near the Mississippi River outflow (D'Sa and

Miller, 2003; Højerslev and Aarup, 2002) reported a strong seasonality induced by the river discharge, and that K_0 depended on the organic and inorganic particle and dissolved yellow substance contents of the waters. Højerslev and Aarup (2002) found that *Zs* in this shelf ranged from a low of < 5 m in water depths ≤ 25 m but increased to over 17 m in deeper waters. Working in the southwest Florida shelf, Højerslev (1985) found *Zs* of over 17 m because of the low freshwater influence and small particle concentrations in this region.

The objectives of this work were to analyze *Zs*, PAR, and transmissometer data spanning two and one-half years (1992 to 1994) over the Louisiana–Texas shelf to provide a description of optical characteristics of these waters. A practical contribution of this work will be revised equations between light attenuation coefficients and *Zs* for the study area. Given that many researchers still employ Secchi disks in this region, the updated equations should be a valuable contribution.

Theoretical considerations.—The theory behind the Secchi disk as an optical sensor begins with the contrast equation for an optically homogeneous water column (Tyler, 1968; Williams, 1970; Preisendorfer, 1986). This equation allows writing the fundamental equation of the Secchi disk as (Tyler, 1968; Holmes, 1970; Williams, 1970; Preisendorfer, 1986)

$$c + K_0 = \frac{\Gamma}{Zs} \qquad (2)$$

where c is the beam attenuation coefficient, Γ is the coupling constant, and the remaining symbols retain their previous meaning. Besides the assumption of a homogeneous column, c and K_0 are average values from the surface to *Zs*, which depend on the sun's angle, the optical properties of pure water, and the organic and inorganic particle and dissolved matter contents of the water. The units of c and K_0 are m^{-1} whereas Γ is a dimensionless number whose value lies between 6 and 9 (Preisendorfer, 1986). The coupling constant depends on the roughness or waviness of the sea surface and the reflectance of skylight. In practice, c is estimated using a transmissometer to record the light beam attenuation over a set distance as the instrument is lowered through the water column. Notice that in Equation 2, K_0 is not related to *Zs* as Equation 1 suggests, but the sum $c + K_0$ is related to *Zs*. Thus, to determine K_0 from *Zs*, c must be known somehow. Krezel and Sagan (1991) indicate that, for wavelengths of 520–540 nm, c and K_0 are directly proportional, i.e., $c \approx \alpha K_0$, which simplifies equation (2) to one similar to equation (1) but with a constant different from Γ.

Oceanographic setting.—Average near-surface currents over the Louisiana–Texas shelf display a two-season pattern that in turn could be subdivided into two spatial regimes (Nowlin et al., 2005). The shelf can be divided into the inner and outer shelf along the 50-m isobath where the zero isotach lies. The annual flow pattern in the inner shelf consists of a downcoast, from Louisiana to Texas, current in nonsummer (Sept.–May) and a reverse flow in summer (June–Aug.). However, the length of these seasons varies interannually. On the outer shelf, currents are upcoast, from Texas to Louisiana, most of the year. The inner-shelf currents are driven primarily by the seasonal wind stress and freshwater input from the Mississippi–Atchafalaya and other minor rivers, whereas the outer-shelf currents are driven primarily by Loop Current rings and other smaller-scale eddies. These circulation patterns and river discharge affect the salinity field. The mean discharge of the Mississippi–Atchafalaya River varies seasonally with a peak discharge ($\sim$ 32,000 $m^3\ s^{-1}$) right before summer, decreases to its minimum at the end of summer ($\sim$ 10,000 $m^3\ s^{-1}$), and increases throughout the nonsummer season. Generally, low salinity waters are found on the inner shelf due to the large input of freshwater, whereas in the outer shelf salinity has near–open ocean values (Nowlin et al., 2005). Near Texas the salinity tends to be low in nonsummer when fresher waters are brought by the downcoast flow, but higher during the summer due to saltier water input by the upcoast flow. Near the Mississippi Delta, salinity tends to be lower in summer due to the piling of fresher water by upcoast currents and increase in nonsummer due to saltier water input by the downcoast flow. In addition to having low salinity, inner-shelf waters tend to have large loads of suspended sediments (Walker and Rouse, 1993). These fresher and turbid inner-shelf waters respond strongly to wind events such that river plumes can be seen over the shelf with tongue-like water masses that can increase the mixing of fresh and saltier waters over the mid- and outer shelf. These winds also push the river water parcels close to the 200-m isobath near the Mississippi Delta (Walker and Rouse, 1993). These tongues and parcels of river water laden with sediments and particles affect the optical properties and their variability over this shelf.

DOI: 10.18785/goms.2601.02

TABLE 1. Dates, number of stations, and season for each cruise employed in this study.

Cruise	Start date	End date	No. of stations	Season
H01	1 May 1992	8 May 1992	114	Summer
H02	1 Aug. 1992	8 Aug. 1992	124	Summer
H03	5 Nov. 1992	13 Nov. 1992	114	Nonsummer
H04	6 Feb. 1993	13 Feb. 1993	119	Nonsummer
H05	26 April 1993	11 May 1993	215	Summer
H06	26 July 1993	7 Aug. 1993	215	Summer
H07	7 Nov. 1993	21 Nov. 1993	238	Nonsummer
H08	24 April 1994	7 May 1994	170	Summer
H09	27 July 1994	4 Aug. 1994	171	Summer
H10	2 Nov. 1994	13 Nov. 1994	170	Nonsummer
Total			1,650	

METHODS

Measurements of *Zs*, PAR, and light transmission used in this work were collected during 10 cruises spanning two and one-half years over the Louisiana–Texas Shelf from May 1992 through November 1994 by scientists from Texas A&M University (Nowlin et al., 1998). Table 1 shows the dates, number of stations, and season for each cruise. The cruises covered the area within longitudes 90.5°W to 97°W and latitudes 26°N to 29°N, encompassing water depths from 10 m to near 1,000 m (Fig. 1). Stations with PAR measurements during the 10 cruises numbered 1,650. Measurements of PAR depend on the sun's angle, which varies seasonally. We accounted for this seasonal variation by selecting those stations occupied when the sun's rays arrive at angles $\leq 60°$ from the vertical. This angle sets the sun's altitude at greater than 30°, which reduces the reflectance to $\leq 6\%$ on a flat sea surface (Jerlov, 1968). The times when the sun's rays arrived at angles $\leq 60°$ from the vertical were calculated as follows: (1) estimate cos(h) as

$$\cos(h) = \frac{\cos(Z) - \sin(\phi)\sin(\delta)}{\cos(\phi)\cos(\delta)}$$

where h is the time angle, Z is the sun's vertical angle ($Z = 60°$), φ is the latitude ($\varphi = 28°$), and δ is the sun's declination obtained, for example, from Byers (1974) and (2) convert the time angle (h) to local time by

$$t = 12 \mp \frac{12 \cdot h}{\pi}$$

where the minus sign is used for morning hours and the plus sign for afternoon hours. Our database consisted of 469 samples after retaining stations with concurrent PAR, transmissometer, and *Zs* measurements, and discarding stations with low sun altitude, no data, and a subsurface light maximum. The seasonality of the circulation and river discharge (Nowlin et al., 1998, 2005) motivated us to divide these data into summer and nonsummer (Fig. 1). The summer fraction consists of 332 stations and nonsummer of 137 stations. These data represent 25 times more data than used by Poole and Atkins (1929) and Holmes (1970).

Secchi depths were measured using a standard disk (30 cm in diameter) lowered into the water with its white surface toward the observer (Jochens et al., 1996). The disk was lowered until just visible and the depth recorded, then lowered until it completely disappeared. The disk was raised until just visible and that depth recorded; the reported *Zs* is the average of these two readings. All measurements were conducted from the shaded side of the ship during daylight hours. Because the cruises were carried on a predetermined and fairly uniform pattern, the *Zs* and other measurements are not random, but they allowed resolving spatial and seasonal variations.

PAR measurements were conducted using a Biospherical QSP-200L scalar irradiance meter (Jochens et al., 1996). The irradiance was measured in micro-Einsteins $m^{-2}\,s^{-1}$ and reported in binned intervals of 0.5 m from about 0.5–3.0 m below the surface to near the bottom. Surface light measurements were not collected. The Secchi disk technique is predicated on the assumption that the water column is optically homogenous between the surface and *Zs*. Analyses of the PAR profiles suggest that in water depths greater than 10 m, two optical layers exist with the upper layer confined to 10 m (unpublished data) similar to observations by Clarke (1938). Thus, we applied an exponential regression to PAR measurements at ≤ 10 m to estimate $K_0 < 10$ as the attenuation coefficient for this

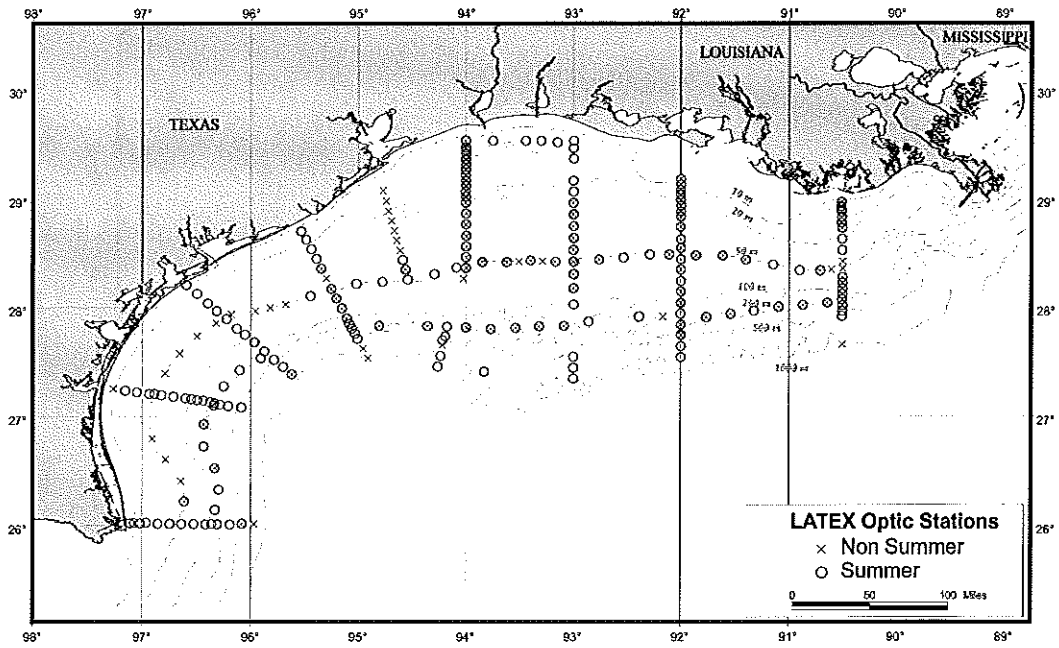

Fig. 1. Location of optical stations over the Louisiana–Texas shelf for summer and nonsummer times. Some of these stations were occupied more than once during the study period (May 1992–Nov. 1994).

layer and satisfy the assumption of homogeneity. This is consistent with Poole and Atkins (1929), who divided the water column from surface to 20 m, 20–40 m, and 40–60 m, but used the 0–20-m data to explore the correlation between K_0 and Zs.

Transmissometer data were collected using a SeaTech 2000 sensor with a 25-cm path length and 660-nm wavelength (Jochens et al., 1996). Data were binned at 0.5 m and reported as percentage of light transmitted over the 25-cm path length. Because this instrument supplies its own light, c is independent of the sun's angles, but it can vary seasonally because of the water's particle contents. The manufacturer indicates that c should be computed as

$$c = \frac{-1}{z}\ln(\textit{light transmission in decimals})$$

where z = 0.25 m in this work, and ln(x) is the natural logarithm. We estimated an average c between the surface and 10 m corresponding with our estimates of K_0 as discussed above. Thus, c and K_0 used in this work represent independent averages over the upper water layer of ≤ 10 m thickness.

Estimates of K_0 and c were paired with the observed Zs along with other information (location, water depth, season, etc.) for each station to construct a database. The database was exported to a geographical information system to produce maps and conduct spatial analyses. Basic statistics (means, maximum, minimum), the 95% confidence level of the mean, and regressions were computed from this database. The confidence interval (CI) of the mean at the 95% confidence level was estimated by the mean ± the confidence level as

$$CI = Y + t_{0.05}\frac{s}{\sqrt{n}}$$

where Y is the mean value, s is the standard deviation and n is the number of observations. The parameter $t_{0.05}$ represents the t-function with n − 1 degrees of freedom, and is between 1.97 and 1.96. A t-test at the 95% confidence level was employed to check the differences of the mean values. Linear regressions between $K_0 + c$, K_0, and c as dependent variables against the reciprocal of Zs were run. Using $1/Zs$ as the independent variable allows using linear regressions instead of curvilinear regressions as this transformation converts the equations employed into linear functions (i.e., y = mx). The regressions should be significant if the data conform to theory, i.e., Equations 2–4. We also plotted c vs K_0 to explore the assumption that these two coefficients are linearly related as in Krezel and Sagan (1991). Regressions were calculated for all, summer, and nonsummer periods respectively. We examined seasonal variations but not interannual variability.

DOI: 10.18785/goms.2601.02

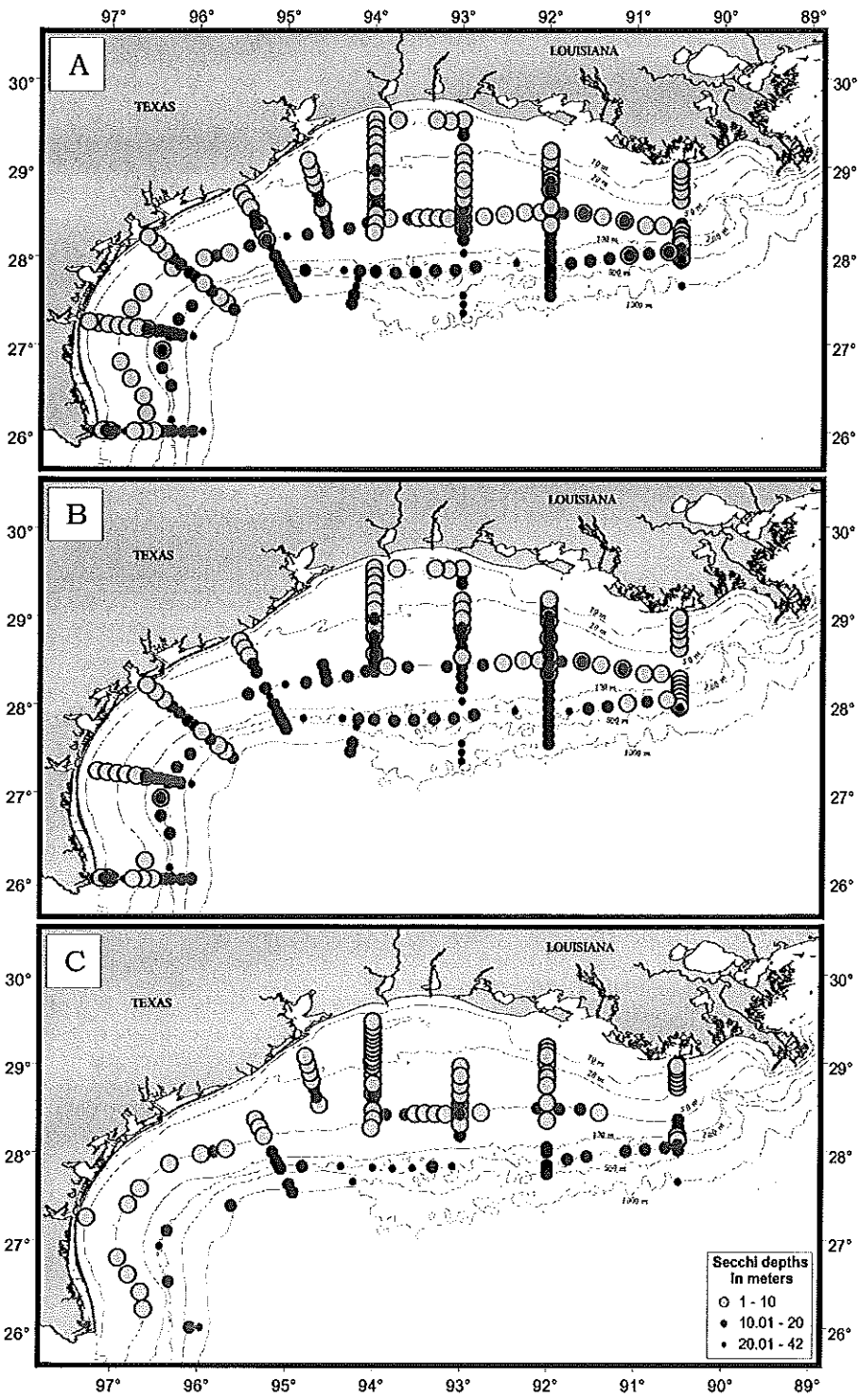

Fig. 2. Maps of Secchi depths (*Zs*) over the Louisiana–Texas shelf divided into all (A), summer (B), and nonsummer (C) times. Note the shallow *Zs* onshore the 50-m isobath suggesting turbid water and the deeper *Zs* offshore the 50-m isobath suggesting relatively clear waters.

TABLE 2. Basic statistics for Secchi depth (Zs), and light attenuation coefficients c, K_0, and $c + K_0$ for depths $\leq$ 10 m for all, summer, and nonsummer.

	All				Summer				Nonsummer			
	Zs (m)	K_0 (1/m)	c (1/m)	$c + K_0$ (1/m)	Zs (m)	K_0 (1/m)	c (1/m)	$c + K_0$ (1/m)	Zs (m)	K_0 (1/m)	c (1/m)	$c + K_0$ (1/m)
Mean	12.64	0.22	0.84	1.06	13.78	0.20	0.76	0.96	9.86	0.25	1.03	1.29
Maximum	42.00	1.18	7.78	8.78	42.00	1.18	7.78	8.78	28.00	1.03	4.68	5.71
Minimum	1.00	0.06	0.38	0.49	1.00	0.06	0.38	0.49	1.00	0.07	0.40	0.52
Confidence level[a]	0.640	0.010	0.070	0.080	0.770	0.010	0.080	0.090	1.060	0.030	0.140	0.170

[a] At the 95% level.

RESULTS

Spatio-temporal variations of optical parameters.—Statistics concerning Zs for all, summer, and nonsummer periods are shown in Table 2. First, Zs ranges from 1 m to 42 m in summer, but only 1 m to 28 m in nonsummer. This table shows that the 95% level CI mean of Zs for all is 12.64 $\pm$ 0.64 m, in summer the CI of the mean Zs is 13.78 $\pm$ 0.77 m, the CI of the mean decreases to 9.86 $\pm$ 1.06 m in nonsummer. The means for summer and nonsummer are statistically different according to the t-test. The largest observed Zs (= 42 m) occurs only once and appears to be an outlier, but it could also indicate that this measurement was made in a very clear water parcel near 50 m.

Maps of Zs for all, summer, and nonsummer times are shown in Figure 2. These maps show that shallower Zs ($\leq$ 10 m) occur inside the 50-m isobath in general. Intermediate Zs (10–20 m) occur off Texas during summer (Fig. 2B). During nonsummer, shallower Zs are confined to inside the 50-m isobath, but some intermediate Zs occur near the Mississippi Delta (Fig. 2C). The deeper Zs (> 20 m) occur offshore the 100-m isobath nearly all the time; exceptions occur during summer when some are found near the 50-m isobath (Fig. 2B). Smaller Zs at depths of 10–50 m suggest a narrow band of very turbid water present during both seasons, whereas the near uniform and larger Zs at depths greater than $\sim$ 100 m indicate relatively clear waters. These values and distribution of Zs agreed with the results of Højerslev and Aarup (2002).

Statistics for K_0, c, and $K_0 + c$ are provided in Table 2 for all, summer, and nonsummer periods. Estimates of K_0 are derived from regressions for which over 90% of them had $r^2 \geq 0.90$ but some had r^2 between 0.80 and 0.54. In summer the 95% CI for the mean K_0 equals 0.20 $\pm$ 0.01 m^{-1} and in nonsummer it is 0.25 $\pm$ 0.03 m^{-1}; this difference is significant according to the t-test. The CI for the overall mean K_0 equals 0.22 $\pm$ 0.01 m^{-1}, and this average is statistically different from the nonsummer average but equal to the summer value according to the t-test. The 95% CI for the mean c in summer is 0.76 $\pm$ 0.08 m^{-1} and 1.03 $\pm$ 0.14 m^{-1} in nonsummer, and again this difference is significant according to the t-test. The CI for the overall mean c equals 0.84 $\pm$ 0.07 m^{-1}, and this average is statistically different from the nonsummer average but equal to the summer value according to the t-test. Jerlov (1968) reports that for "fairly turbid waters" $c \sim 0.89$ m^{-1} at 660 nm and we adopt this value as a reference point. These data show that 58% of nonsummer stations fall inside the 50-m isobath where the water is very turbid and one should expect $c \geq 0.89$ m^{-1}. In summer, the data reveal that about 50% of the stations fall offshore of the 50-m isobath where the water is clearer and one should expect $c <$ 0.89 m^{-1}, which is exactly what we found. The 95% CI for the mean $c + K_0$ in summer equals 0.96 $\pm$ 0.09 m^{-1} and 1.29 $\pm$ 0.17 m^{-1} in nonsummer, and this difference is significant according to the t-test. The CI for the overall mean $c + K_0$ equals 1.06 $\pm$ 0.08 m^{-1}, and this average is statistically equal to the summer value according to the t-test. Furthermore, in summer at the inner shelf K_0 = 0.25 m^{-1} and K_0 = 0.16 m^{-1} at the outer shelf; the inner shelf c = 0.99 m^{-1} and, at the outer shelf, c = 0.68 m^{-1}. In nonsummer, the inner shelf K_0 = 0.31 m^{-1} and K_0 = 0.16 m^{-1} at outer shelf; in the inner shelf c = 1.60 m^{-1} and, at the outer shelf, c =0.54 m^{-1}. The outer-shelf K_0 remains nearly steady year round, but c differs; at the inner shelf both K_0 and c change.

Regression analysis.—Regressions of $c + K_0$ vs $1/Zs$ for all, summer, and nonsummer times are shown in Figure 3. As expected, the plot exhibits a linear relationship as suggested by Equation 2. The 95% CIs show that the regression constants are significantly different from zero. The coupling constants ranged from 6.8 to 7.5 which agree with Preisendorfer (1986). The difference between summer and nonsummer is statistically significant on the basis of the 95% CIs. The coupling constant for all and the summer are not different according to the 95% CIs.

DOI: 10.18785/goms.2601.02

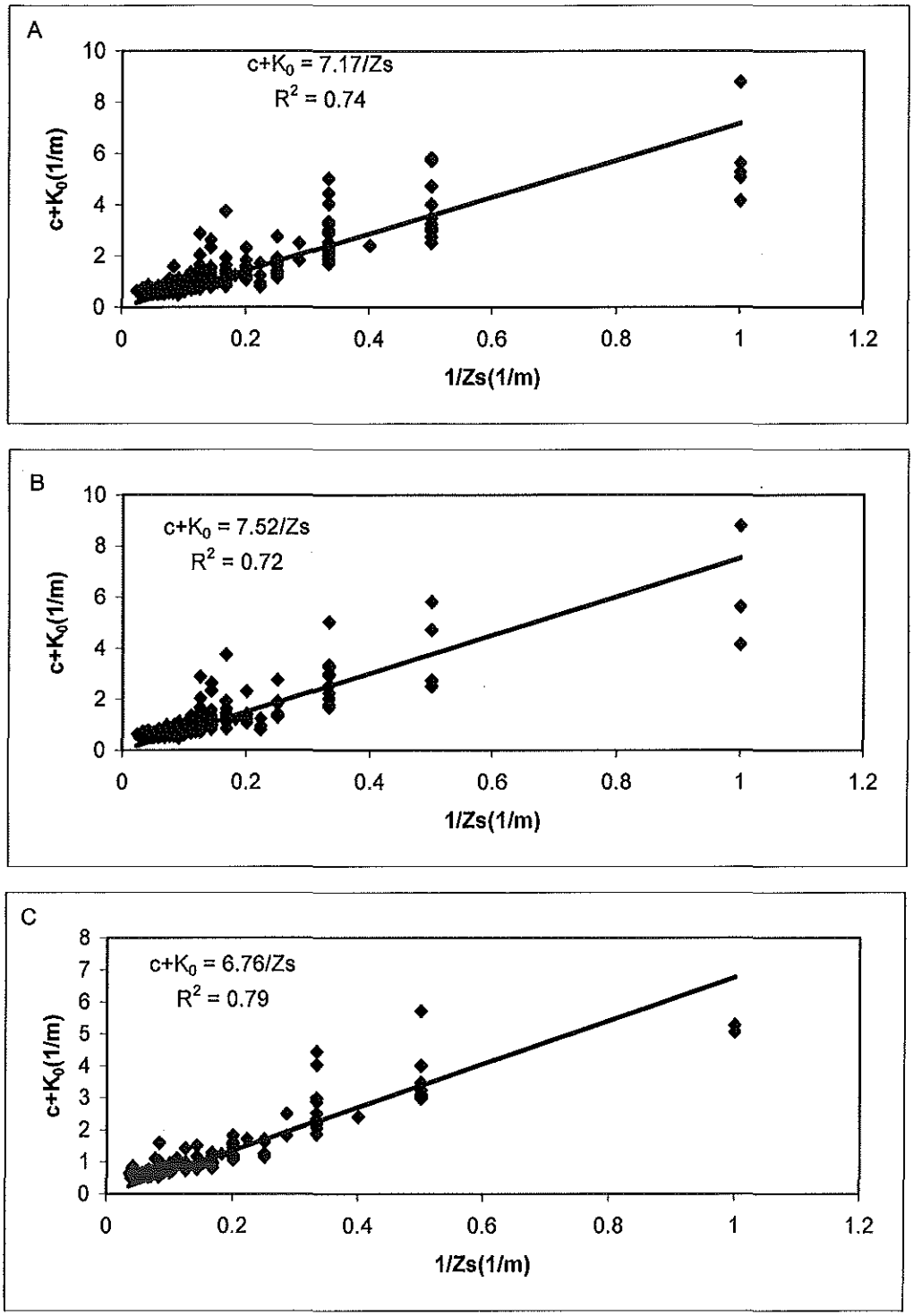

Fig. 3. Regressions between the light attenuation coefficients, $c + K_0$, for depths $\leq$ 10 m against the reciprocal of Zs for all (A), summer (B), and nonsummer (C). These regressions are significant and explain 72–79% of the variability.

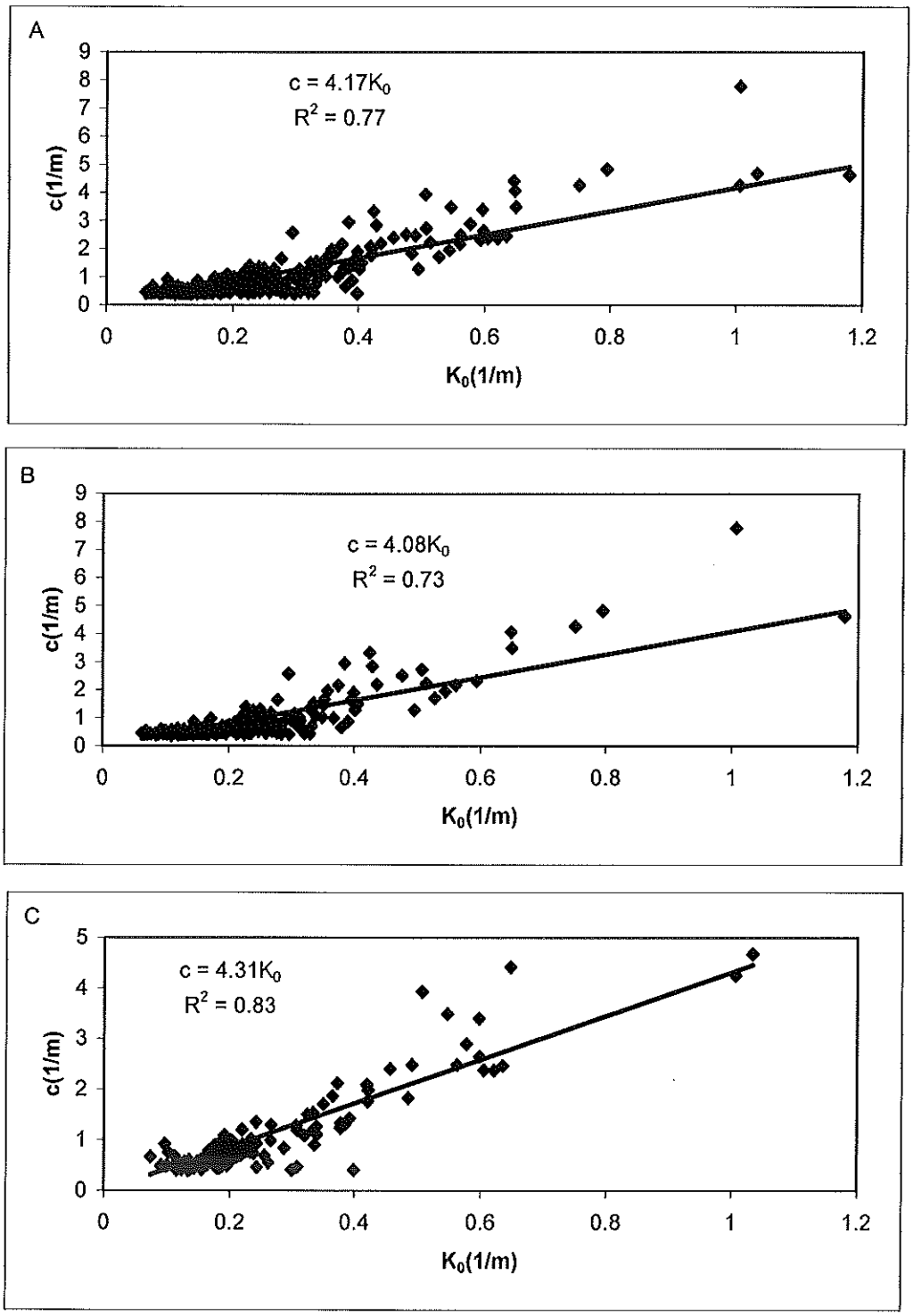

Fig. 4. Regressions between light attenuation coefficients, c vs K_0 for depths ≤ 10 m for all (A), summer (B), and nonsummer (C). These regressions are significant and explain 73–83% of the variability.

DOI: 10.18785/goms.2601.02

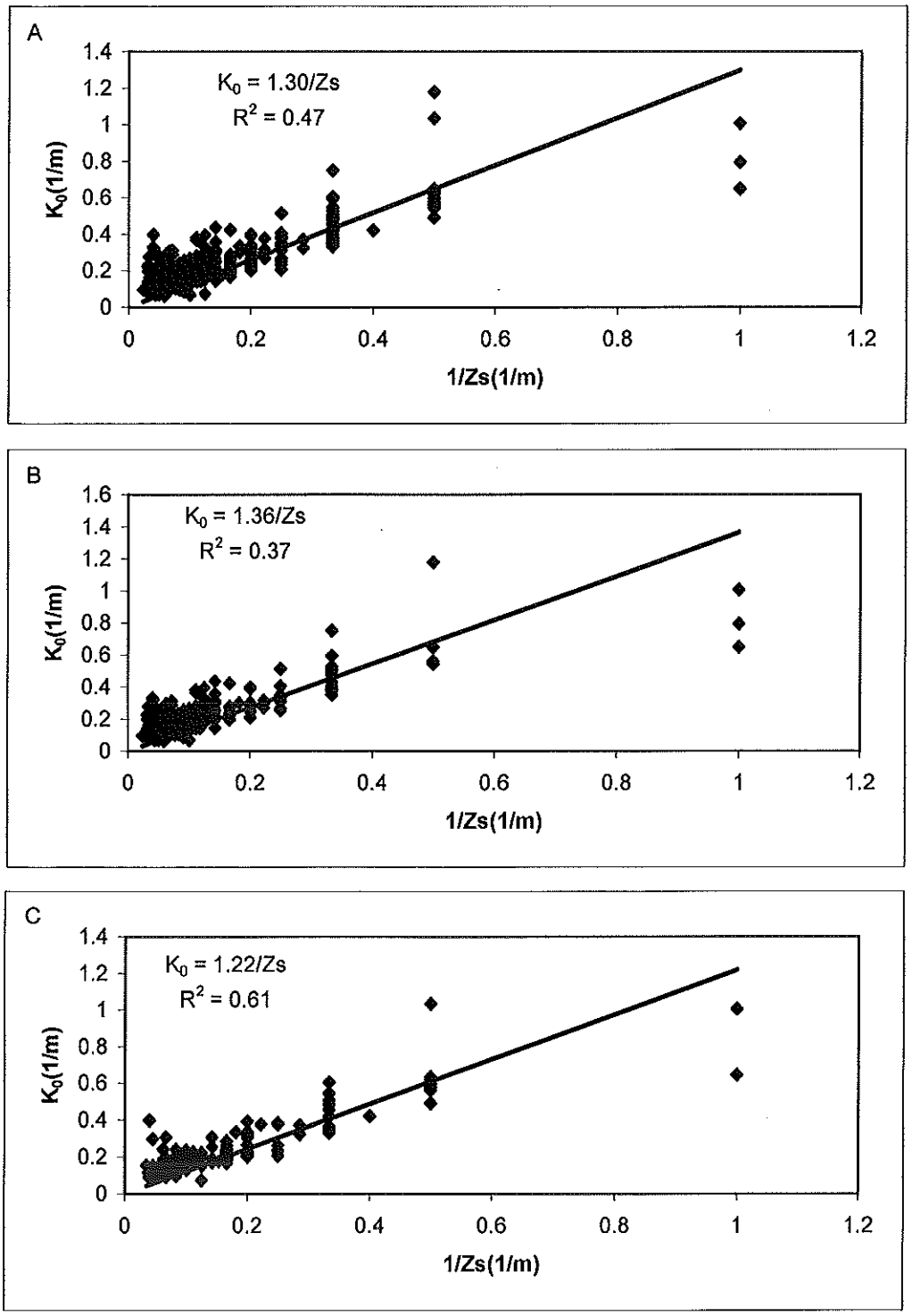

Fig. 5. Regressions between the light attenuation coefficient, K_0, for depths ≤ 10 m against the reciprocal of *Zs* for all (A), summer (B), and nonsummer (C). These regressions are significant and explain 37–61% of the variability.

Because the transmissometer wavelength (660 nm) falls outside the range where c and K_0 are proportional (Krezel and Sagan, 1991), we tested whether these coefficients are still directly proportional. We plotted c vs K_0 in Figure 4, for all, summer and nonsummer times. Figure 4A, the all case, reveals that indeed c and K_0 are directly proportional. The proportionality constant equals 4.17 and is significantly different from zero according to the 95% CI. Summer and nonsummer cases (Fig. 4B, C), confirmed the linear relation between these two coefficients with proportionality constants of 4.08 and 4.31, respectively. The proportionality constants for summer and nonsummer are statistically equal according to the 95% CI. Although these regressions explain 73% to 83% of the variance, these seem to be a deviation from a line especially for the summer data (Fig. 4B). This aspect will be explored later.

Because c and K_0 are statistically directly proportional, we proceeded to substitute this into Equation 2 and reduced it to

$$K_0 = \frac{B}{Zs} \quad (3)$$

which means that K_0 is inversely proportional to Zs with a proportionality constant B given by $\frac{\Gamma}{1+\alpha}$ (Γ is the coupling constant and α is the proportionality constant between c and K_0). Figure 5, showing K_0 vs $1/Zs$, confirms that Equation 3 is satisfied by the data. Although the regression constants are statistically different from zero according to the 95% CI, they do not explain very much (37–61%) of the K_0 variance.

The linear dependence between K_0 and c allows Equation 2 to be solved for c as

$$c = \frac{C}{Zs} \quad (4)$$

which means that c is inversely proportional to Zs with a proportionality constant C given by $\frac{\Gamma\alpha}{1+\alpha}$ (symbols retain their previous meaning). Figure 6, showing c vs $1/Zs$, confirms that Equation 4 is satisfied by these data. The regression constants are statistically different from zero according to the 95% CI, and the regressions explain a higher (72–79%) percentage of c's variance.

Finally, the regressions in Figures 3 and 4 were employed to predict B and C in Equations 3 and 4. Table 3 shows the values of Γ, α, B, and C predicted and estimated from the observations. The agreement is very good, with errors less than 10%, but always underpredicting B and overpredicting C, which suggests small but consistent biases.

Discussion

The high biological productivity of the Louisiana–Texas shelf affects and is affected by optical conditions of these waters. The particle load (inorganic and organic) and its distribution by the oceanographic circulation are major controllers of optical conditions. Particle loads are driven by sunlight, nutrients, productivity, and sediment input. The shelf's circulation is driven by winds, freshwater input, and offshore mesoscale features. All these driving forces, except mesoscale features, exhibit seasonal cycles that induce similar variability in the optical parameters. Besides these reasons, our focus on seasonal variations stems from the fact that two and one-half years of data provide a greater likelihood of successfully separating the seasonal signal than do the annual variations. We sought to remove the sun's seasonal effects by selecting records during high solar altitudes. Previous studies (Gordon, 1989; Mishra et al., 2005) have found that K_0 is nearly independent of the sun's altitude for angles $\leq$ 40° and that changes in incident solar radiation do not significantly affect K_0. Thus, in setting $Z \leq 60°$ the astronomical seasonal variation in the data was eliminated or minimized. This selection criterion affected the data distribution between summer and nonsummer. Six cruises were in summer and four in nonsummer and, additionally, the lower sun altitude in nonsummer further reduced the nonsummer sample size such that summer sample size was about two and one-half times higher than nonsummer. This sample size difference helps explain the similarity of the statistics between overall and summer.

The predetermined patterns of the cruises prevent randomness in Zs measurements, but they allow detection of temporal and spatial variations. The sampling patterns also introduced two potential errors in the observations. First, making observations from the shaded side could introduce large errors in Zs (Tyler, 1968). However, our results are consistent with previous reports and theory, leading us to conclude that this error is negligible. Secondly, Zs measurements were made in the presence of waves, which is against recommended practice.

We evaluated wave effect as Højerslev (1985) suggests, but using seasonal wave height averages. The resulting errors are 20% to 60% underestimation of Zs, which will have a net effect of increasing the constants in the regressions as the dependent variables (K_0 and c) remain unaltered. However, this correction was not adopted because it is not commonly used and will prevent comparison with previous reports that do not correct for this effect.

DOI: 10.18785/goms.2601.02

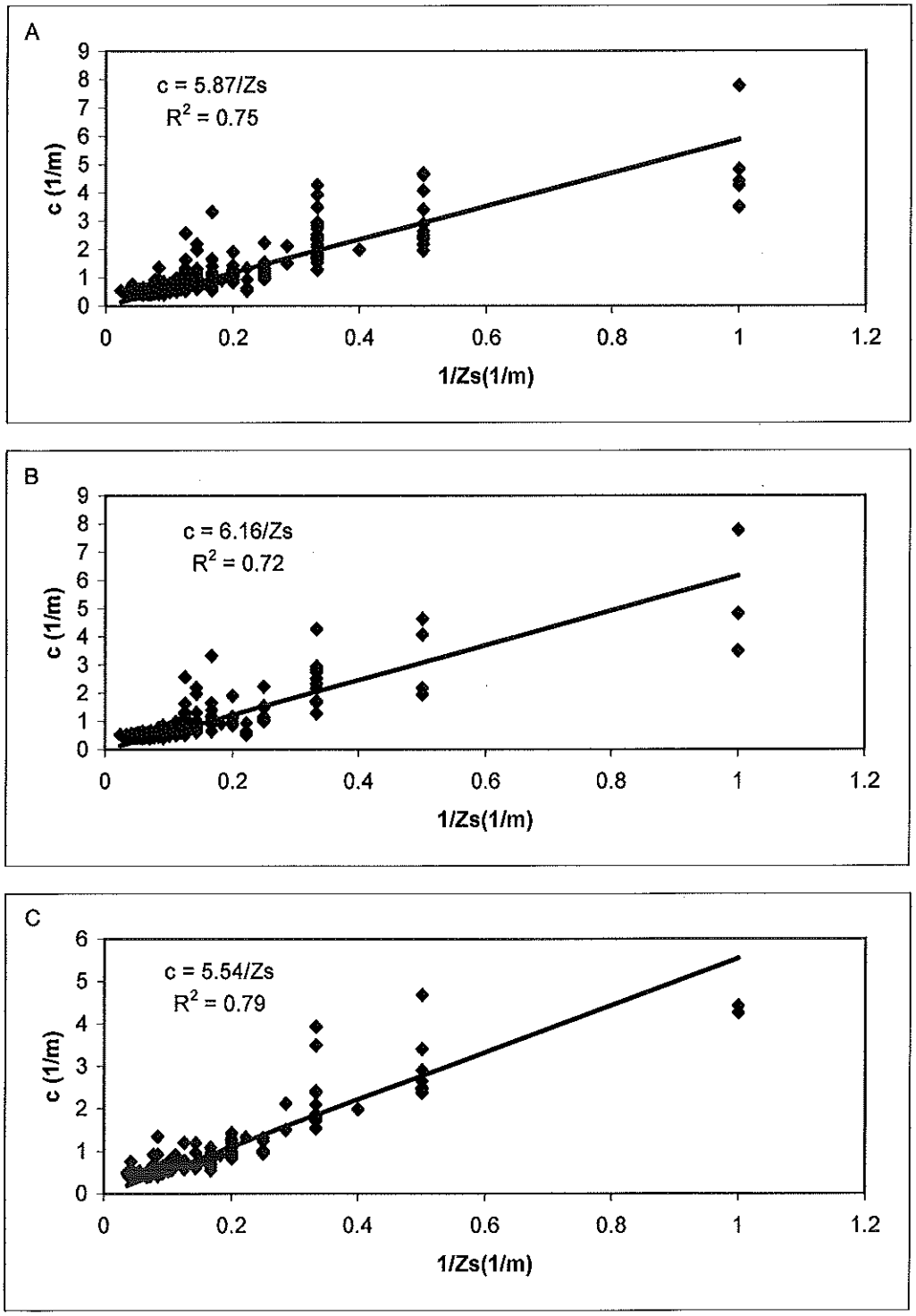

Fig. 6. Regressions between the light attenuation coefficient, c, for depths ≤ 10 m against the reciprocal of Zs for all (A), summer (B), and nonsummer (C). These regressions are significant and explain 72–79% of the variability.

TABLE 3. Estimates of the proportionality constant for Equations 3 and 4 from the regression coefficients, note the small but biased errors for B and C. The variables Γ, α, B, and C retain their previous meanings.

	Γ	α	B predicted	B estimated	Error	C predicted	C estimated	Error
All	7.17	4.17	1.39	1.30	−6.26	5.78	5.87	1.50
Summer	7.52	4.08	1.48	1.36	−8.13	6.04	6.16	1.99
Nonsummer	6.76	4.31	1.27	1.22	−4.17	5.49	5.54	0.97

Secchi depths presented in Figure 2 reveal a significant temporal and spatial variation. Temporarily, the mean *Zs* vary from 14 m in summer to 10 m in nonsummer and this difference is statistically significant. Spatially, *Zs* shows great variation inside the 50-m isobath where it ranges from 1 to 30 m; in the outer shelf (depths > 50 m) *Zs* ranges from 10 to 30 m. Similar observations were reported by Højerslev and Aarup (2002), who examined optical measurements along a cross-shelf transect in the study area over 1-yr duration. This observed distribution of *Zs* coincides with the fact that the circulation and particle load in the study area change around 50 m. Nowlin et al. (1998) report that shallower waters are influenced by the Mississippi–Atchafalaya discharge with high particle loads and winds, whereas deeper waters are mostly under the influence of offshore processes that consist mostly of clear waters.

The optical coefficients K_0 and c vary temporally and spatially, but these variations are opposite that of *Zs* as the equations indicate. Both K_0 and c are greater in nonsummer than in summer, indicating greater light penetration in summer. Both coefficients tend to be larger onshore of 50 m or the inner shelf, but smaller offshore of the 50-m isobath or outer shelf, again indicating less penetration in the inner shelf than in the outer shelf. These seasonal and spatial variations are related to the shelf's seasonal circulation and freshwater input. The inner-shelf, nonsummer large attenuation coefficients reflect high inputs of freshwater (recall that river discharge peaks this season) with large particle loads that are distributed along the cost by the downcoast flow current regime. Furthermore, particle increase is caused by sediment resuspension by higher winds in the inner shelf. In summer, the freshwater input decreases and the upcoast current piles the water near the Mississippi Delta bringing clearer water from offshore by continuity close to shore, especially offshore of south Texas. Weaker winds also cause low sediment resuspension on average in the inner shelf. These seasonal differences tend to induce smaller *Zs* or higher K_0 and c in the inner shelf. Spatially, this seasonal change should induce large *Zs* in summer near Texas and smaller *Zs* in the east but our data (Fig. 2B, C) do not verify this inference of an east–west gradient. In the outer shelf the circulation regime is mostly upcoast year round, and under the influence of the deep Gulf mesoscale features, which bring clear water with low particle loads, K_0 and c are smaller. However, water parcels from the inner shelf are transported to the outer shelf bringing turbid water and thus creating variability in the optical conditions. Deslarzes and Lugo-Fernández (2007) observed such changes near the shelf edge. Curl's (1959) estimates of K_0 over the northeastern Gulf of Mexico, based on 1 yr of data, ranged from 0.15 m^{-1} to 0.45 m^{-1} for the inner shelf and about 0.15 m^{-1} for the offshore areas. He could not detect seasonal trends or salinity effects. We speculate that these significant differences are caused by changes of particle loads over the shelf, which in turn are caused by changes in circulation and freshwater. Nowlin et al. (1998) report high particle concentrations in the inner shelf but lower in the outer shelf. Again, these results agree with Højerslev and Aarup (2002).

The regression analyses showed that in summer the equations relating K_0 and c to *Zs* are

$$c + K_0 = \frac{7.52}{Zs} \quad c = 4.08K_0$$

$$K_0 = \frac{1.36}{Zs} \quad c = \frac{6.16}{Zs}$$

In nonsummer the regression equations are

$$c + K_0 = \frac{6.76}{Zs} \quad c = 4.31K_0$$

$$K_0 = \frac{1.22}{Zs} \quad c = \frac{5.54}{Zs}$$

The results of this work show that the simple Equation 1 (Poole and Atkins, 1929) for K_0 in waters of the Louisiana–Texas shelf needs to be

DOI: 10.18785/goms.2601.02

modified because the coefficient differs and varies with season, a result that agrees with Krezel and Sagan (1991) and Holmes (1970). These constants are different from the value of 1.7 found by Poole and Atkins (1929) and commonly suggested in textbooks, e.g., Parsons et al. (1984) and Sverdrup et al. (1942). Curl (1959) found that B = 1.68 for offshore water in the northeastern Gulf and quoted a report of B = 1.43 for waters in a harbor, whereas Holmes (1970) found that B = 1.44. However, this result differs from Idso and Gilbert (1974), who found that Equation 1 is valid even in turbid waters. The values for the constants in Equation 3 are very similar to those found by Holmes (1970) and Curl (1959). This study is similar to that conducted by Poole and Atkins (1929) in the sense that we employed K_0 values estimated from light measurements in the upper layer to ensure a homogenous water layer and measurements of Zs from the shaded side of the ship. But unlike Poole and Atkins (1929), Holmes (1970), and Idso and Gilbert (1974) we employed data spanning two and one-half years amounting to 469 points, which greatly exceeds their databases. The greater number of points ensures robust results with a high degree of statistical significance. Højerslev and Aarup (2002) derived a constant of 1.88, but they used a normalized Zs to correct for wave effects, which were not accounted for in this study.

It was mentioned earlier that Figure 4B hinted that the linear relation between c and K_0 was weak, especially at high K_0. This deviation is small because the linear regression accounts for 73% of the variance in Figure 4B and 83% in Figure 4C. This aspect was explored using nonlinear regressions. A quadratic polynomial did improve the r^2 values by 1–6%, which is not significant given the increase in degrees of freedom. Other functions, e.g., exponential, logarithmic, or power, did not did well either. So, if there are nonlinearities, these appear to be small and to first approximation, c and K_0 are related linearly. However, the surprising result is that Equation 3 or Figure 5 explains only 37–61% of the variance, whereas Equation 4 or Figure 6 accounts for 72–79% of the variance. Because the deviations from a line occur at high K_0 values or in the inner shelf, this suggests that we are missing an important factor contributing to high values of K_0. Perhaps the high sediment loads in the inner shelf are introducing nonlinearities, or it could be because of the colored dissolved matter. For practical applications, it is suggested that Equations 2 and 4 be used and K_0 determined by subtraction.

Summarizing, we provide updated equations to estimate K_0 and c from measurements of Zs that account for seasonal changes. However, we caution that the preferred method to estimate the attenuation coefficients should employ downwelling irradiance meters and transmissometers as Preisendorfer (1986) recommends.

Acknowledgments

The authors appreciate the support of the U.S. Department of the Interior, Minerals Management Service, Gulf of Mexico OCS Region during the preparation of this manuscript. The opinions expressed by the authors are their own and do not reflect the opinion or policy of the U.S. government.

Literature Cited

Byers, H. R. 1974. General meteorology. McGraw-Hill, Inc., New York.

Clarke, G. L. 1938. Light penetration in the Caribbean Sea and in the Gulf of Mexico. J. Marine Res. 1:85–94.

Curl, H., Jr. 1959. The hydrography of the inshore northeastern Gulf of Mexico. Publ. Inst. Mar. Sci., Univ. Texas 6:193–205.

Deslarzes, K. J. P., and A. Lugo-Fernández. 2007. Influence of terrigenous runoff on offshore coral reefs: an example from the Flower Garden Banks, Gulf of Mexico, p. 126–160. *In:* Geological approaches to coral reef ecology: placing the current crises in historical context. Ecological studies 192. R. B. Aronson (ed.). Springer Verlag, New York.

D'Sa, E., and R. L. Miller. 2003. Bio-optical properties in waters influenced by the Mississippi River during low flow conditions. Remote Sens. Environ. 84: 538–549.

Gordon, H. R. 1989. Can the Lambert–Beer law be applied to the diffuse attenuation coefficient of ocean water? Limnol. Oceanogr. 34(8):1389–1409.

Højerslev, N. K. 1985. Bio-optical measurements in the southwest Florida shelf ecosystem. J. Cons. Int. Explor. Mer., 4265–85.

———, and T. Aarup. 2002. Optical measurements on the Louisiana shelf off the Mississippi River. Estuar. Coast. Shelf Sci. 55:599–611.

Holmes, R. W. 1970. The Secchi disk in turbid coastal waters. Limnol. Oceanogr. 15(5):688–694.

Idso, S. B., and R. G. Gilbert. 1974. On the universality of the Pool and Atkins Secchi disk-light extinction equation. J. Appl. Ecol. 11(1):399–401.

Jerlov, N. G. 1968. Optical oceanography. Elsevier Oceanography Series, New York.

Jochens, A. E., D. A. Wiesenburg, L. E. Sahl, C. N. Lyons, and D. A. DeFreitas. 1996. LATEX shelf data report: hydrography, April 1992 through November 1994. Texas A&M Oceanography Dept., Texas A&M Univ., Technical Report 96-6-T.

Krezel, A., and S. Sagan. 1991. Relation between Secchi disk depth and light attenuation coefficient

c(525 nm) in water of the Gulf of Gdansk. Mar. Phys. Pol. Acad. Sci. 6:183–196.

MISHRA, D. R., S. NARUMALANI, D. RUNDQUIST, AND M. LAWSON. 2005. Characterizing the vertical diffuse attenuation coefficient for downwelling irradiance in coastal waters: implications for water penetration by high resolution satellite data. J. Photogrammetry Remote Sens. 60(1):48–64.

NOWLIN, W. D., A. E. JOCHENS, S. F. DIMARCO, R. O. REID, AND M. K. HOWARD. 2005. Low-frequency circulation over the Texas–Louisiana continental shelf, p. 219–240. *In:* Circulation in the Gulf of Mexico: observations and models. AGU Monograph 161. W. Sturges and A. Lugo-Fernández (eds.). American Geophysical Union, Washington, DC.

———, ———, R. O. REID, AND S. F. DIMARCO. 1998. Texas–Louisiana shelf circulation and transport process study: synthesis report LATEX A. Volume I and II. OCS Study MMS 98-0035 and MMS 98-0036. U.S. Dept. of the Interior, Minerals Management Service, Gulf of Mexico OCS Regional Office, New Orleans.

PARSONS, T. R., M. TAKAHASHI, AND B. HARGRAVE. 1984. Biological oceanographic processes Pergamon Press Ltd., New York.

POOLE, H. H., AND W. G. R. ATKINS. 1929. Photo-electric measurements of submarine illumination throughout the year. J. Mar. Biol. Assoc. U. K. 16(1):297–324.

PREISENDORFER, R. W. 1986. Secchi disk science: visual optics of natural waters. Limnol. Oceanogr. 31(5): 909–926.

SANDEN, P., AND B. HÅKANSSON. 1996. Long-term trends in Secchi depth in the Baltic Sea. Limnol. Oceanogr. 41(2):346–351.

SMITH, R. C., AND K. S. BAKER. 1984. The analysis of ocean optical data. Ocean Optics VII, SPIE 478:119–126.

SVERDRUP, H. U., M. W. JOHNSON, AND R. H. FLEMING. 1942. The oceans, their physics, chemistry, and general biology. Prentice-Hall, New York.

TYLER, J. E. 1968. The Secchi disc. Limnol. Oceanogr. 13(1):1–6.

WALKER, N. D., AND L. J. ROUSE. 1993. Satellite assessment of Mississippi River discharge plume variability. OCS Study MMS 93-0044. U.S. Dept. of the Interior, Minerals Management Service, Gulf of Mexico OCS Regional Office, New Orleans.

WILLIAMS, J. 1970. Optical properties of the sea. U.S. Naval Institute, Annapolis, MD.

(AL-F) PHYSICAL SCIENCES UNIT (MS 5433), 1201 ELMWOOD PARKWAY BOULEVARD, NEW ORLEANS, LOUISIANA 70123-2394; AND (MG, TM) MAPPING AND AUTOMATION UNIT (MS 5413), 1201 ELMWOOD PARKWAY BOULEVARD, NEW ORLEANS, LOUISIANA 70123-2394. Date accepted: August 22, 2008.

DOI: 10.18785/goms.2601.02